

# TOWARDS RECONSTRUCTING THE FINAL STAGE OF HEAVY ION COLLISIONS<sup>1</sup>

Urs Achim Wiedemann

*Institut für Theoretische Physik, Universität Regensburg,  
D-93040 Regensburg, Germany*

## Abstract

A Fourier inversion problem lies at the heart of determining spatio-temporal characteristics of the final stage of a heavy ion collision: From the measured two-particle momentum correlations  $C(\mathbf{p}_1, \mathbf{p}_2)$  of identical particles, pions say, a Hanbury-Brown /Twiss (HBT) interferometric analysis aims at extracting as much information as possible about the Wigner phase space density  $S(x, p)$  of pion emitting sources in the collision region, [1, 2]

$$C(\mathbf{q}, \mathbf{K}) = 1 + \frac{|\int d^4x S(x, K) e^{ix \cdot q}|^2}{\int d^4x S(x, p_1) \int d^4y S(y, p_2)}, \quad (1)$$

where  $q = p_1 - p_2$ ,  $K = \frac{1}{2}(p_1 + p_2)$ . Here, we discuss how the analysis of (1) allows to separate the effects of temperature and transverse flow which cannot be disentangled completely on the basis of single-particle spectra.

---

<sup>1</sup>Paper presented at the XXXIIth Rencontres de Moriond, “QCD and High Energy Hadronic Interactions”, Les Arcs, France, March 22-29, 1997.

Physics is rich in Fourier inversion problems which are not analytically invertible. A well-known example is the determination of the charge density distribution  $\rho(\mathbf{r})$  of atomic nuclei from the structure function  $F(\mathbf{q})$  measured in elastic electron scattering,

$$F^2(\mathbf{q}) = \left| \frac{1}{e} \int d\mathbf{r} \rho(\mathbf{r}) e^{i\mathbf{q}\mathbf{r}} \right|^2. \quad (2)$$

In most cases, this structure function was measured only in a small window of the momentum transfer  $\mathbf{q}$  which makes an analytical unfolding of  $\rho(\mathbf{r})$  without additional assumptions impossible. The standard way out is to take recourse to model distributions  $\rho(\mathbf{r})$  like e.g. the Fermi distribution  $\rho(\mathbf{r}) = \rho_0 / \left(1 + \exp(\frac{\mathbf{r}-R}{z})\right)$  whose parameters have a simple physical interpretation. In a first step, these model parameters are determined in a fit of  $F(\mathbf{q})$ , till a refined analysis reveals the need for more detailed models which include e.g. dips in the charge distribution for small  $\mathbf{r}$ , cf. [3].

In our analysis of the measured two-particle correlations (1), we adopt essentially the same strategy, for different reasons though: the detected pions which determine  $C(\mathbf{q}, \mathbf{K})$  are on mass-shell and this results in a constraint for the relative pair momentum  $q$ ,  $q \cdot K = 0$ . Hence, the four-vector  $q$  has only three independent components and even for an exactly known correlator, the Fourier transform (1) is not uniquely invertible. This necessitates a model-dependent approach.

The analysis presented here is based on a model pion emission function including resonance decay channels  $R$ :

$$S_\pi(x, p) = S_\pi^{\text{dir}}(x, p) + \sum_R S_{R \rightarrow \pi}(x, p). \quad (3)$$

The contributions  $S_{R \rightarrow \pi}$  are obtained from the direct resonance emission function  $S_R^{\text{dir}}(X, P)$  by propagating the resonances of widths  $\Gamma$ , produced at  $(X_\mu, P_\mu)$ , along a classical path  $x^\mu = X^\mu + \frac{P^\mu}{M}\tau$  according to an exponential decay law [4, 5, 6]:

$$S_{R \rightarrow \pi}(x, p) = \int_{\mathbf{R}} \int d^4X \int d\tau \Gamma e^{-\Gamma\tau} \delta^{(4)}\left(x - \left(X + \frac{P}{M}\tau\right)\right) S_R^{\text{dir}}(X, P), \quad (4)$$

where  $\int_{\mathbf{R}}$  is the integral over the available resonance phase space for isotropic decays. Our model assumes local thermalization at freeze-out and produces hadronic resonances by thermal excitation. For particle species  $i$  with spin degeneracy  $2J_i + 1$ , the emission function reads [6]

$$S_i^{\text{dir}}(x, P) = \frac{2J_i+1}{(2\pi)^3} P \cdot n(x) \exp\left(-\frac{P \cdot u(x) - \mu_i}{T}\right) \exp\left(-\frac{r^2}{2R^2} - \frac{\eta^2}{2(\Delta\eta)^2} - \frac{(\tau - \tau_0)^2}{2(\Delta\tau)^2}\right). \quad (5)$$

The Boltzmann factor  $\exp[-(P \cdot u(x) - \mu_i)/T]$  implements both the assumption of thermalization, with temperature  $T$  and chemical potential  $\mu_i$ , and collective expansion with hydrodynamic flow 4-velocity  $u_\mu(x)$ . The geometrical extension of the collision region is determined by Gaussian widths  $R$  and  $\Delta\eta$  in the transverse radius  $r$  and the space-time rapidity  $\eta = \frac{1}{2} \ln[(t+z)/(t-z)]$ , as well as a Gaussian average around a mean freeze-out proper time  $\tau_0$  with dispersion  $\Delta\tau$ . Freeze-out occurs along proper time hyperbolas  $P \cdot n(x) = M_\perp \cosh(Y - \eta)$  where  $Y$  and  $M_\perp$  are the rapidity and transverse mass associated with  $P$ . In the longitudinal direction we assume scaling expansion,  $v_l = z/t$  or  $\eta_l = \frac{1}{2} \ln[(1+v_l)/(1-v_l)] = \eta$ , for the transverse expansion a linear rapidity profile:

$$\eta_t(r) = \eta_f \left(\frac{r}{R}\right). \quad (6)$$

We include all pion decay channels of  $\rho$ ,  $\Delta$ ,  $K^*$ ,  $\Sigma^*$ ,  $\omega$ ,  $\eta$ ,  $\eta'$ ,  $K_S^0$ ,  $\Sigma$  and  $\Lambda$  with branching ratios larger than 5 percent.

For a given model emission function, both the two-particle spectrum (1) and the one-particle spectrum  $E_p dN/d^3p = \int d^4x S(x, p)$  is determined. On the LHS of Fig. 1, we plot the rapidity ( $y$ ) integrated pion transverse mass spectrum

$$\frac{dN_\pi}{dm_\perp^2} = \int dy \int d^4x S(x, p) \quad (7)$$

for two sets of source parameters without ( $\eta_f = 0$ ) and with ( $\eta_f = 0.3$ ) transverse flow. Note that the geometric parameters  $R$ ,  $\Delta\eta$ ,  $\tau_0$  of the source enter only in the normaliza-

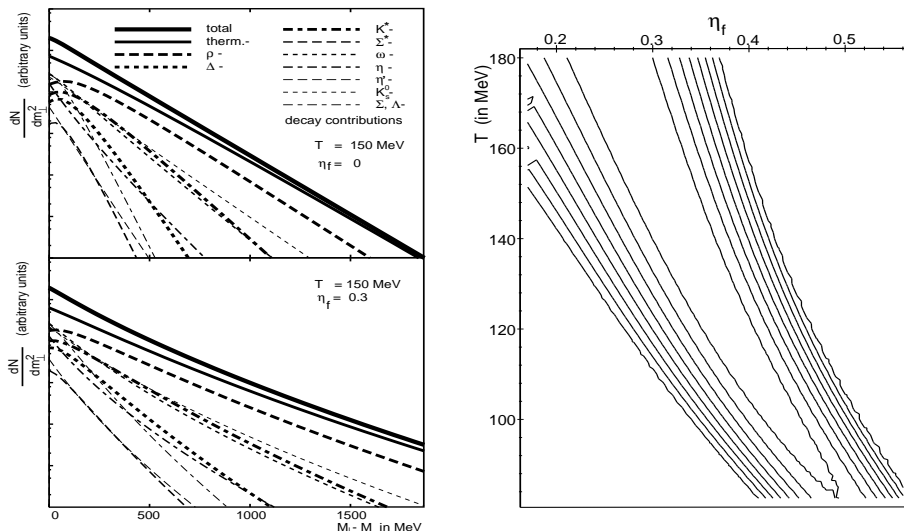


Figure 1: **Left:** One pion transverse momentum spectra according to (7) for different values of the transverse flow  $\eta_f$ . **Right:** The  $\sigma$ -confidence levels for a fit of our model to the NA49  $h^-$ -spectrum at midrapidity.

tion of this spectrum. The slope is essentially determined by the temperature  $T$  and the transverse flow  $\eta_f$  and contains no information on the source geometry. The direct pions reflect essentially an effective “blueshifted” temperature  $T_{\text{eff}} = T \sqrt{\frac{1+\langle\beta_t\rangle}{1-\langle\beta_t\rangle}}$ . If resonance contributions to (7) are included, these statements change in many details, most notably, resonance contributions lead to a low  $p_T$ -enhancement, and a more pronounced flattening of the spectra for larger transverse flow. The main message however remains unaltered: the unnormalized one-particle spectra (7) contain no geometrical information, their slope determines only a combination of temperature and transverse flow. This is clearly seen on the RHS of Fig. 1 where we show the confidence levels of a fit to the NA49  $h^-$ -spectrum [7].

Two-particle correlations are often analyzed in terms of the Gaussian ansatz

$$C(\mathbf{q}, \mathbf{K}) = 1 + \lambda e^{-R_s^2 q_s^2 - R_o^2 q_o^2 - R_l^2 q_l^2 - R_{ol}^2 q_o q_l} . \quad (8)$$

They allow to disentangle temperature and flow effects. To see this, one can consider e.g. the approximate expression

$$R_s^2(K_\perp) \approx \frac{R^2}{1 + (m_\perp/T)\eta_f^2} . \quad (9)$$

Here, the  $m_{\perp}$ -dependence of (9) is governed by a prefactor  $\eta_f^2/T$ . This indicates that the side radius  $R_s(K_{\perp})$  may allow to distinguish scenarios with a relative large temperature and a small transverse flow size  $\eta_f$  from those with a large  $\eta_f$  and small  $T$  which according to the RHS of Fig. 1 account for realistic transverse momentum slopes equally well. We hasten to remark however that (9) is obtained in a crude saddle point approximation neglecting all resonance decay contributions - it is known to be quantitatively unreliable. This was one of our main motivations for a quantitatively accurate, numerical calculation [6] of the two-particle correlation  $C(\mathbf{q}, \mathbf{K})$  and its Gaussian widths.

Most notably, resonance decay contributions can lead to deviations of the correlator from a Gaussian shape. This is a consequence of the exponential resonance decay law and can lead to significant quantitative ambiguities in analyses based on (8), see e.g. the different Gaussian fits depicted in Fig. 2. We hence suggest [6] to characterize the correlator by a set of so-called  $q$ -variances which do not depend on any assumption about the shape. For a unidirectional analysis of the correlations  $\tilde{C}(q_i, \mathbf{K}) \equiv C(q_i, q_{j \neq i} = 0, \mathbf{K})$  along the three Cartesian axes, these  $q$ -moments read

$$R_i^2(\mathbf{K}) = \frac{1}{2 \langle\langle q_i^2 \rangle\rangle}, \quad (10)$$

$$\langle\langle q_i^2 \rangle\rangle = \frac{\int dq_i q_i^2 [\tilde{C}(q_i, \mathbf{K}) - 1]}{\int dq_i [\tilde{C}(q_i, \mathbf{K}) - 1]}, \quad (11)$$

$$\lambda_i(\mathbf{K}) = (R_i(\mathbf{K})/\sqrt{\pi}) \int dq_i [\tilde{C}(q_i, \mathbf{K}) - 1]. \quad (12)$$

Note that for a correlator of Gaussian shape, these expressions coincide with those of a fit to (8). Still, they are well-defined for arbitrary shapes of the correlator. Deviations from a Gaussian shape can be discussed in terms of higher  $q$ -moments, most easily in terms of the “kurtosis”

$$\Delta_i = \frac{\langle\langle q_i^4 \rangle\rangle}{3 \langle\langle q_i^2 \rangle\rangle^2} - 1. \quad (13)$$

Fig. 2 shows the numerically obtained results for the side radius if resonance decay contri-

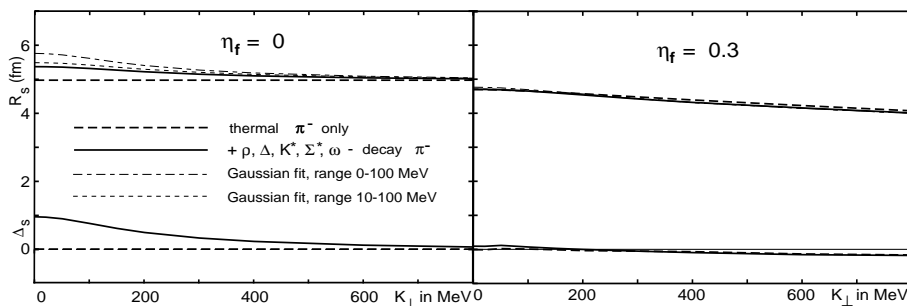


Figure 2: HBT radius parameters  $R_s$  and the kurtosis  $\Delta_s$  calculated from the  $q$ -moments and compared to a Gaussian fit to (8). The two plots depict scenarios without ( $\eta_f = 0$ ) and with ( $\eta_f = 0.3$ ) transverse flow.

butions are added:  $R_s$  develops a  $K_{\perp}$ -slope even for scenarios without transverse flow. The reason is that the resonances propagate outside of the thermally equilibrated region before decaying. This “lifetime effect” leads to exponential tails in  $S_{R \rightarrow \pi}$  and tends to increase the Gaussian widths  $R_i$ . Since the relative abundance of resonances is larger for small  $K_{\perp}$ , this

tail is more pronounced in the region of small  $K_{\perp}$ , thereby leading to a  $K_{\perp}$ -slope of  $R_s$ . In contrast, for a finite transverse flow  $\eta_f = 0.3$  the  $K_{\perp}$ -dependence of  $R_s$  is due to the flow, and resonance decay contributions do not change the slope of  $R_s$  in our model. This can be traced back to a shrinking transverse size of the direct resonance emission function  $S_R^{dir}$  which for the case depicted in Fig. 2, counterbalances the lifetime effect almost exactly [6].

Here, the main message is that resonance decay contributions can lead to a  $K_{\perp}$ -slope of  $R_s$ , even in scenarios without transverse flow, i.e., they are faking a signal previously attributed to transverse collective dynamics. However, the physical origin of the  $K_{\perp}$ -slope of  $R_s$  is different for the two scenarios in Fig. 2 and it is well understood [6] that this physical difference manifests itself in a much more prominent “non-gaussicity” for the case  $\eta_f = 0$ . The kurtosis (13) allows for a quantitative measure of deviations from a Gaussian shape and hence it provides at least for the class of models discussed here, the cleanest distinction between scenarios with and without transverse flow. We hence expect that in a detailed analysis of two-particle correlation functions, based on Eqs. (10)-(13), the effects of temperature and transverse flow can be disentangled most clearly.

In this short presentation, we have focussed entirely on one aspect, the distinction between thermal excitation and transverse collective dynamics in the collision region. We conclude by pointing out that various other geometrical and dynamical characteristics of the source are accessible via the analysis of two-particle correlations. Especially, we mention information on the longitudinal expansion, emission time and emission duration as well as the longitudinal and transverse size of the boson emitting region. In the context of the model (5), resonance decay contributions to these characteristics are quantitatively under control and we are currently working on the determination of the model parameters of (5) from the data [7] taken by the NA49 Collaboration.

This report is based on joint work with Ulrich Heinz. It was supported by BMBF, DFG, GSI and DPNC.

## References

- [1] E. Shuryak, Phys. Lett. **B44**, 387 (1973).
- [2] S. Chapman and U. Heinz, Phys. Lett. **B340**, 250 (1994).
- [3] R. Hofstadter, Ann. Rev. Nucl. Sci. **7**, 231 (1957).
- [4] B.R. Schlei e.al., Phys. Lett. **B293**, 275 (1992); *ibidem* **B376**, 212 (1996).
- [5] H. Heiselberg, Phys. Lett. **B379**, 27 (1996).
- [6] U.A.Wiedemann and U. Heinz, nucl-th/9610043 and nucl-th/9611031.
- [7] P. Foka for the NA49 Collaboration, these proceedings.